Synthesis and Phase Behavior of New Cholesteric Liquid-Crystalline Copolymers Containing Chiral Mesogenic Groups Derived from Menthol Derivatives

Jian-She Hu, Shi-Chao Ren, Bao-Yan Zhang, Chun-Ying Chao

Center for Molecular Science and Engineering, College of Science, Northeastern University, Shenyang 110004, People's Republic of China

Received 28 September 2007; accepted 19 January 2008
DOI 10.1002/app.28045
Published online 2 May 2008 in Wiley InterScience (www.interscience.wiley.com).

ABSTRACT: The synthesis of a new chiral mesogenic monomer ($\mathbf{M_1}$), a nematic monomer ($\mathbf{M_2}$), and a series of side chain cholesteric copolymers ($\mathbf{P_2}$–$\mathbf{P_6}$) containing the mesogenic menthyl groups is described. The chemical structures of the compounds were confirmed by FTIR and ^{1}H NMR. The mesomorphic properties and phase behavior were investigated by differential scanning calorimetry, thermogravimetric analysis, and polarizing optical microscopy. $\mathbf{M_1}$ showed an enantiotropic cholesteric phase, and $\mathbf{M_2}$ revealed a nematic phase. The homopolymers $\mathbf{P_1}$ and $\mathbf{P_7}$, respectively, displayed a chiral smectic A (S_A) phase and a nematic phase, while the copolymers $\mathbf{P_2}$–$\mathbf{P_6}$ exhibited the Grandjean texture of the cholesteric phase. T_g, T_i, and ΔT of $\mathbf{P_1}$–$\mathbf{P_7}$ increased with increasing the concentration of $\mathbf{M_2}$ in the polymers. All of the obtained polymers displayed very good thermal stability and the wide mesophase temperature range. © 2008 Wiley Periodicals, Inc. J Appl Polym Sci 109: 2187–2194, 2008

Key words: chiral; menthyl; liquid-crystalline polymers; cholesteric; nematic; smectic

INTRODUCTION

Both from a scientific and a commercial point of view, cholesteric liquid-crystalline polymers (LCPs)[1–16] have attracted much interest due to their unique optical properties, including the selective reflection of light, thermochromism and circular dichroism, and their potential applications such as reversible optical storage, full-color thermal imaging, and electro-optical materials. Chirality can be introduced in LCPs at various levels and located in the terminal position of the pendant mesogenic units. The rod-like, chiral molecules responsible for the macroscopical alignment of the mesogenic domains can produce a cholesteric phase. Depending on the chemical structure, it may be feasible to achieve a macroscopic alignment of the cholesteric phase domains. Many side-chain cholesteric LCPs, mostly adopting commercially available chiral compounds such as cholesterol and (*S*)-(+)-2-methyl-1-butanol, have been studied.[17–23] They were usually prepared by the copolymerization of a nematic monomer and a chiral mesogenic monomer or a chiral nonmesogenic monomer.[19,24]

Menthol derivatives have been used as a nonmoesgenic chiral monomer for the synthesis of side-chain cholesteric LCPs.[25–32] However, to the best of our knowledge, research on chiral liquid-crystalline (LC) monomers and polymers containing mesogenic menthyl groups was not seen. Liu and Yang[32] reported synthesis and characterization of novel monomers and polymers containing chiral (−)-menthyl groups. Although these chiral monomers, containing two or three phenyl rings, had good rigidity and tended to reveal mesophase, their mesogenic cores were directly linked to menthyl groups, thus the existence of the bulky steric hindered menthyl group that disturbed the arrangement of chiral monomers leading to the disappearance of LC phases.

We found that the compounds containing menthyl groups could form and exhibit LC phases (such as smectic, cholesteric, or blue phase) when a flexible spacer was inserted between the mesogenic core and the menthyl groups to reduce the steric hindered effect, it is similar to the decouple effect same as a flexible spacer inserted between the polymeric main chain and the mesogenic side groups. The aims of our research are as follows: (i) to study structure–property relationships of new chiral LC monomers and polymers containing mesogenic menthyl groups; (ii) to supply the necessary data to synthesize piezoelectric and ferroelectric LC materials; and (iii) to explore their advanced applications. In this study, a new chiral LC

Correspondence to: B.-Y. Zhang (baoyanzhang@hotmail.com).

Contract grant sponsors: National Natural Science Foundation of China, Natural Science Foundation of Liaoning Province, Program for New Century Excellent Talents (NCET) in University.

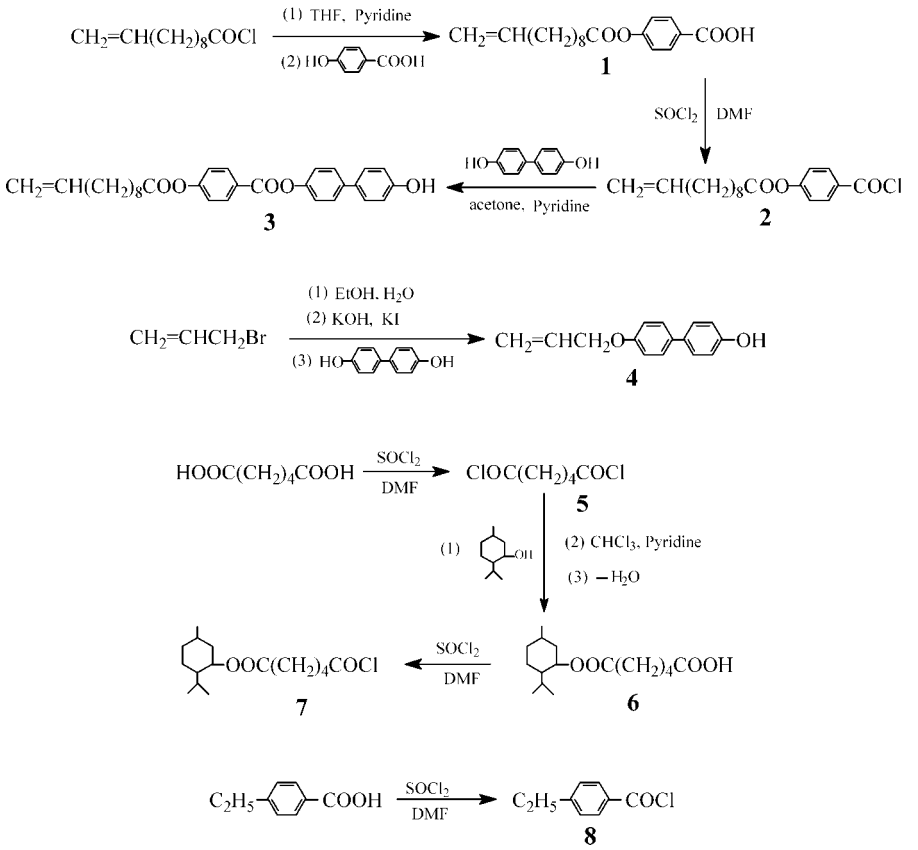

Scheme 1 Synthesis of the intermediate compounds.

monomer, a nematic monomer and a series of side-chain cholesteric polysiloxanes containing mesogenic menthyl groups were prepared and characterized. The mesomorphic properties and phase behavior of the monomers and polymers obtained were investigated with differential scanning calorimetry (DSC), thermogravimetric analysis (TGA), and polarizing optical microscopy (POM). The effect of copolymerization composition on the phase behavior is discussed.

EXPERIMENTAL

Materials

Polymethylhydrosiloxane (PMHS, M_n = 700–800) was purchased from Jilin Chemical Industry (Jilin, China). 4,4′-Dihydroxybiphenyl (from Aldrich, Beijing, China) was used as received. 4-Hydroxybenzoic acid was purchased from Beijing Fuxing Chemical Industry (Beijing, China). 4-Ethylbenzoic acid was purchased from Beijing Chemical Reagent (Beijing, China). Undecylenic acid was purchased from Beijing Jinlong Chemical Reagent (Beijing, China). Menthol was purchased from Shanghai Kabo Chemical (Shanghai, China). Toluene used in the hydrosilylation reaction was purified by treatment with $LiAlH_4$ and distilled before use. All other solvents and reagents were purified by standard methods.

Measurements

FTIR spectra were measured on a Perkin–Elmer spectrum One (B) spectrometer (Perkin–Elmer, Foster City, CA). ^{1}H NMR (400 MHz) spectra were obtained with a Varian WH-90PFT spectrometer (Varian Associates, Palo Alto, CA). The optical rotations were obtained on a Perkin-Elmer 341 polarimeter. The phase transition temperatures and thermodynamic parameters were determined with a Netzsch DSC 204 (Netzsch, Germany) equipped with a liquid nitrogen cooling system. The heating and cooling rates were 10°C/min. The thermal stability of the polymers under nitrogen atmosphere was measured with a Netzsch TGA 209C thermogravimetric analyzer. The heating rates were 20°C/min. A Leica DMRX POM (Leica, Germany) equipped with a Linkam THMSE-600 (Linkam, England) cool and hot stage was used to observe the phase transition temperatures and analyze the mesomorphic properties through the observation of optical textures.

Synthesis of the intermediate compounds

The synthetic route of the intermediate compounds is outlined in Scheme 1. Yields, structural characterization, and some physical properties of the inter-

TABLE I
Yield, Melting Temperatures, and IR Characterization of Intermediate Compounds

Compounds	Yield (%)	Recrystallized solvent	T_m (°C)	IR (KBr) (cm^{-1})
1	76	Ethanol	130	3300–2500 (—COOH); 2975, 2852 ($-CH_2-$); 1754, 1684 (C=O); 1643 (C=C); 1602, 1508 (—Ar)
3	49	Acetone	178	3378 (—OH), 2921, 2849 ($-CH_2-$), 1754, 1730 (C=O), 1642 (C=C), 1602, 1508 (Ar—)
4	51	Ethanol/acetone (2 : 1)	176	3401 (—OH); 1642 (C=C); 1609, 1512 (—Ar); 1246 (C—O—C)
6	57	Ethyl acetate	140	3300–2500 (—COOH); 2959, 2874 (CH_3-, $-CH_2-$); 1751, 1687 (C=O)

mediate compounds are summarized in Table I. 4-(10-Undecylen-1-yloxy)benzoic acid (**1**) and 4-hydroxybiphenyl-4′-(10-undecylen-1-yloxy)benzoate (**3**) were prepared according to the method reported previously.[33–35]

4-Allyloxy-4′-hydroxybiphenyl (4)

4,4′-Dihydroxybiphenyl (18.6 g, 0.1 mol) were dissolved in 100 mL of ethanol, and then potassium hydroxide (11.2 g, 0.2 mol), 0.5 g of potassium iodide, and 30 mL of water were added. After dropwise addition of 8.2 mL of allyl bromide, the mixture was refluxed for 24 h under stirring. The mixture was poured into a 1000-mL beaker filled with 5% sodium hydroxide solution, and then hot filtered. The crude product was precipitated by acidification of the filtrate and recrystallized from ethanol. White crystal was obtained.

Menthyloxycarbonylvaleric acid (6)

Adipyl chloride **5** was prepared through the reaction of adipic acid with excess thionyl chloride according to the similar reported literature.[35] The solution of menthol (15.6 g, 0.1 mol) in 50 mL of chloroform and 8 mL of pyridine was added dropwise to compound **5** (91.5 g, 0.5 mol) dissolved in 300 mL of chloroform under quick stirring. The mixture was reacted for 5 h at room temperature, and then heated to reflux for 20 h. After removing the solvent by rotatory evaporate, the residue was poured into a beaker filled with 500 mL of ice water. This mixture was stirred for 1 h, filtrated, and the crude product was washed several times with warm water, and then recrystallized from ethyl acetate. White solid was obtained.

Synthesis of the monomers

The synthetic route to olefinic monomers is shown in Scheme 2.

4-(10-Undecylen-1-yloxybenzoyloxy)biphenyl-4′-menthyloxycarbonylvalerate (M_1)

Menthyloxycarbonylvaleryl chloride **7** was obtained through the reaction of compound **6** with excess thionyl chloride according to the similar reported literature.[35] The acid chloride **7** obtained (6.06 g, 0.02 mol) was dissolved in 10 mL of chloroform, and then added dropwise to a solution of compound **3** (9.44 g, 0.02 mol) in 120 mL of chloroform and 20 mL of pyridine under stirring. The mixture was reacted at room temperature for 5 h and refluxed for 40 h, and cooled to room temperature and then filtered. After the filtrate was concentrated, the crude product was precipitated by adding methanol to the filtrate, and then recrystallized from ethanol/acetone (3 : 1). Yield 65%. $[\alpha]_D^{20}$ −25.4° (toulene). IR (KBr, cm^{-1}): 3072 (=C—H); 2927, 2851 ($-CH_3$, $-CH_2-$); 1761, 1736, (C=O); 1642 (C=C); 1605, 1498 (Ar—). ^1H NMR ($CDCl_3$, TMS, δ, ppm): 0.93–2.25 [m, 42H, $-(CH_2)_8-$, $-OOC(CH_2)_4COO-$ and menthyl-***H***); 4.08 (m, 1H, ($COOCH<$ in menthyl); 4.94–5.06 (m, 2H, CH_2 =CH—); 5.76–5.88 (m, 1H, CH_2=C***H***—); 7.13–8.14 (m, 12H, Ar—***H***).

4-Allyloxybiphenyl-4′-ethylbenzoate (M_2)

4-Ethylbenzoyl chloride **8** was obtained through the reaction of 4-ethylbenzoic acid with excess thionyl chloride according to the similar reported literature.[35] The acid chloride **8** obtained (8.5 g, 0.05 mol) was dissolved in 10 mL of tetrahydrofuran (THF), and then added dropwise to a solution of compound **4** (11.3 g, 0.05 mol) in 100 mL of THF and 4 mL of

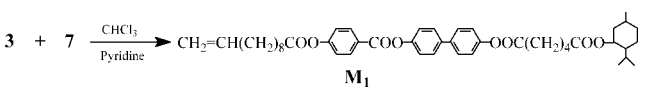

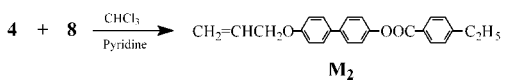

Scheme 2 Synthesis of the LC monomers.

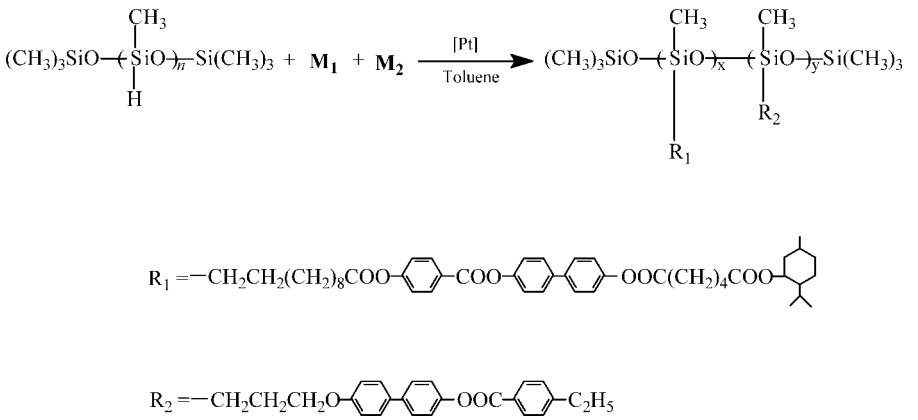

Scheme 3 Synthesis of the LC polymers.

pyridine. The reaction mixture was refluxed for 24 h and cooled to room temperature. After the mixture was concentrated, the rest was poured into cold water. The crude product obtained was washed with water and hot ethanol, and then purified by recrystallization from acetone. Yield 71%. IR (KBr, cm^{-1}): 3037 (=C—H); 2964, 2875 (—CH_3, —CH_2—); 1735 (C=O); 1641 (C=C); 1609, 1501 (Ar—). ^{1}H NMR ($CDCl_3$, TMS, δ, ppm): 1.39–1.50 (m, 3H, —C***H***$_3$); 2.63 (m, 2H, —C***H***$_2$$CH_3$); 4.62 (d, 2H, =CHC***H***$_2$O—); 5.25–5.40 (m, 2H, C***H***$_2$ =CH—); 6.02–6.15 (m, 1H, CH_2 =C***H***—); 6.90–8.07 (m, 12H, Ar—***H***).

Synthesis of the polymers

The synthesis of the polymers $\mathbf{P_1}$–$\mathbf{P_7}$ is shown in Scheme 3. All were synthesized through the hydrosilylation reaction, the synthesis of $\mathbf{P_3}$ is presented as an example. $\mathbf{M_1}$, $\mathbf{M_2}$, and **PMHS**, fed in Table II, were dissolved in freshly distilled toluene. The reaction mixture was heated to 60°C under nitrogen and anhydrous conditions, and then 3 mL of THF solution of H_2PtCl_6 catalyst (5 mg/mL) was injected with a syringe. The progress of the hydrosilylation reaction, monitored from the Si—H stretch intensity, went to completion, as indicated by IR. $\mathbf{P_3}$ was obtained and purified by several reprecipitations from toluene solution into methanol, and then dried in vacuum. IR spectra of $\mathbf{P_3}$ showed the complete disappearance of the Si—H stretching band at 2166 cm^{-1} and olefinic C=C stretching band at 1642 cm^{-1}. Characteristic Si—O—Si and Si—C stretching bands appeared at 1300–1000 cm^{-1}. In addition, the absorption bands of the ester C=O and aromatic still existed.

TABLE II
Polymerization and Yield

Polymers	Feed (mmol)			$\mathbf{M_2}$[a] (mol %)	Yield (%)
	PMHS	$\mathbf{M_1}$	$\mathbf{M_2}$		
$\mathbf{P_1}$	0.50	3.50	0.00	0	89
$\mathbf{P_2}$	0.50	3.15	0.35	5	92
$\mathbf{P_3}$	0.50	2.80	0.70	10	90
$\mathbf{P_4}$	0.50	2.10	1.40	20	91
$\mathbf{P_5}$	0.50	1.40	2.10	50	90
$\mathbf{P_6}$	0.50	0.70	2.80	80	92
$\mathbf{P_7}$	0.50	0.00	3.50	100	93

[a] Molar fraction of $\mathbf{M_2}$ based on ($\mathbf{M_1}$ + $\mathbf{M_2}$).

RESULTS AND DISCUSSION

Phase behavior of the monomers

The phase behavior of the monomers $\mathbf{M_1}$ and $\mathbf{M_2}$ was investigated with DSC and POM. Their phase transition temperatures and corresponding enthalpy changes, obtained on the second heating and the first cooling scans, and mesophase types are summarized in Table III. Representative DSC thermograms of $\mathbf{M_1}$ and $\mathbf{M_2}$ are presented in Figures 1 and 2.

According to Figures 1 and 2, $\mathbf{M_1}$ and $\mathbf{M_2}$ showed a melting transition at 101.7 and 133.5°C, and a LC to isotropic phase transition at 155.7 and 221.9°C on heating cycle, respectively. On cooling cycle, an isotropic to cholesteric phase transition and crystallization temperature for $\mathbf{M_1}$ appeared at 152.6 and 77.8°C, respectively; an isotropic to nematic phase transition and crystallization temperature for $\mathbf{M_2}$ occurred at 190.7 and 90.3°C, respectively.

TABLE III
Phase Transition Temperature (°C) and Enthalpy Changes (J/g) of Monomers

Monomers	Heating cycle	Cooling cycle
$\mathbf{M_1}$	K101.7(46.7)Ch155.7(1.1)I	I152.6(1.2) Ch77.8(36.7)K
$\mathbf{M_2}$	K133.5(87.9)N221.9(3.3)I	I190.7(1.9) N90.3(27.4)K

K, solid; Ch, cholesteric; N, nematic; I, isotropic.

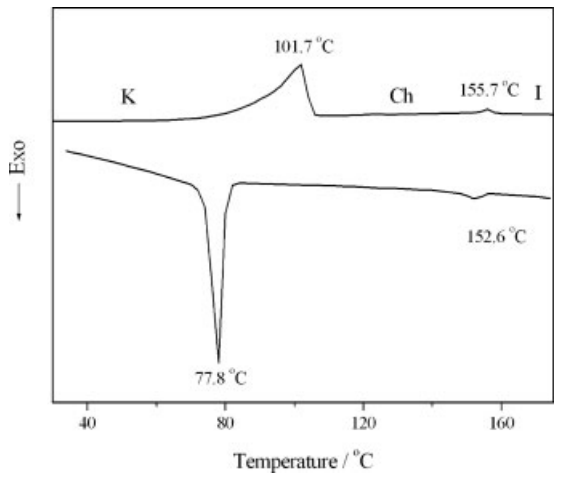

Figure 1 DSC thermograms of $\mathbf{M_1}$.

In general, cholesteric LC at zero field exhibits two optically contrasting stable states: planar (including oily-streak, Grandjean, and fingerprint) texture and focal-conic texture, when cholesteric phase is in the planar texture, the helical axis is perpendicular to the cell surface, the material Bragg-reflects colored light; when cholesteric phase is in the focal-conic texture, the helical axis is more or less parallel to the cell surface, the material is forward-scattering and does not appear selective light reflection. The optical textures of the LC monomers obtained were observed by POM with a hot stage. POM results showed that $\mathbf{M_1}$ displayed enantiotropic cholesteric phase on heating and cooling cycles. When $\mathbf{M_1}$ was heated to 101°C, the sample began to melt, and then typical cholesteric appeared gradually. Heating was continued and the oily streak texture was transformed into finger print texture. The mesomorphic properties and texture disappeared at 158°C. When the isotropic state was cooled to 157°C, the cholesteric focal conic appeared, and crystallized at 72°C.

In nematic phase, the long molecular axes of the molecules orient more or less parallel to each other, while their centers of mass are isotropically distributed. So the nematic phase exhibits solely long-range orientational order. Nematics between untreated glass plates often orient with their director parallel to the substrates. In general, nematic thread-like and schlieren textures are observed under planar boundary conditions.

When $\mathbf{M_2}$ was heated to 133°C, nematic-threaded texture and schlieren texture appeared, and LC behavior disappeared at 224°C. When the isotropic state was cooled to 197°C, the nematic droplet texture firstly appeared and gradually changed to threaded texture, and crystallized at 87°C. Optical textures of $\mathbf{M_1}$ and $\mathbf{M_2}$ are shown in Figure 3(a–c).

Phase behavior of the polymers

The phase behavior of side-chain LCPs depends on the nature of the polymer backbone, the length of the mesogenic core, the flexible spacer, and the copolymer composition. The mesogens are usually attached to the polymer backbone through the flexible spacer. The polymer backbone and mesogens have antagonistic tendencies as follows: the polymer backbone is driven toward a random coil-type configuration, whereas the mesogens stabilize with long-range orientational order. The flexible spacer, which is in general an aliphatic hydrocarbon chain containing, normally, more than two methylene units, decouples the mesogenic side groups from the polymer backbone and renders the mesogens to orientational-order.

The phase transition temperatures and mesomorphic properties of polymers $\mathbf{P_1}$–$\mathbf{P_7}$, obtained with DSC, POM, and TGA, are summarized in Table IV. All phase transitions were reversible and do not change on repeated heating and cooling cycles. The phase transition temperatures determined by DSC were consistent with POM results.

DSC thermograms of $\mathbf{P_2}$–$\mathbf{P_7}$ showed a glass transition at low temperature and a LC to isotropic phase transition at high temperature. However, DSC curve of $\mathbf{P_1}$ only showed a glass transition, and no obvious LC to isotropic phase transition was seen. The reason is that bigger viscosity of LCPs and weaker and slower orientational ability. But POM results showed that $\mathbf{P_1}$ exhibited good mesomorphic properties.

The glass transition temperature (T_g) and the clearing temperature (T_i) of LCPs are very important parameters in connection with structures and properties. For $\mathbf{P_2}$–$\mathbf{P_6}$, because of the same polymer backbone, the corresponding T_g and T_i mainly depended on the copolymer composition (such as the rigidity of the mesogenic unit and the length of the flexible

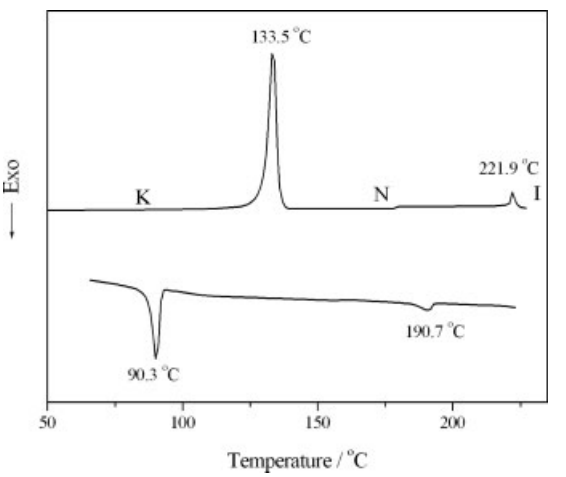

Figure 2 DSC thermograms of $\mathbf{M_2}$.

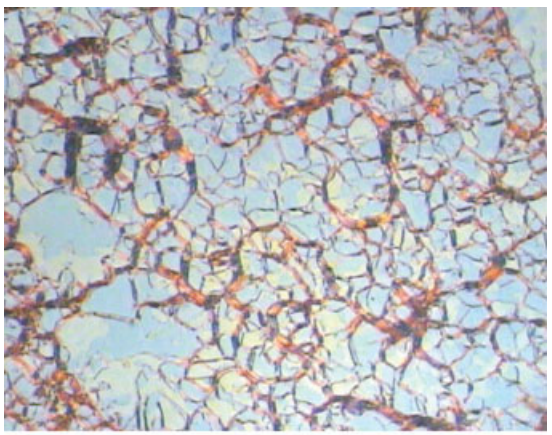

(a)

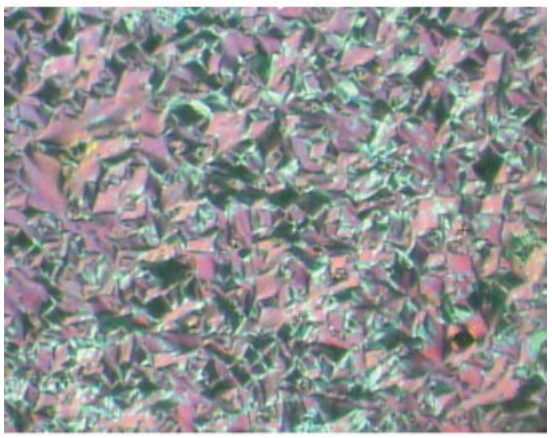

(b)

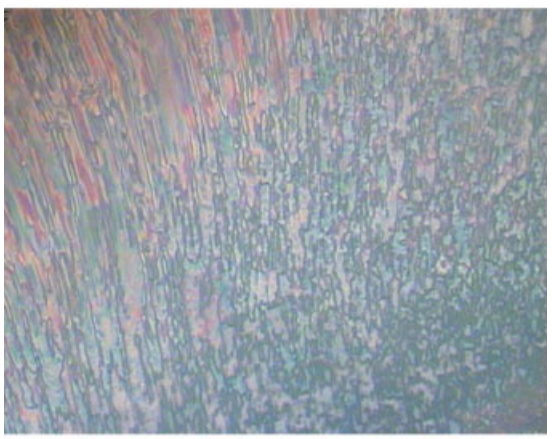

(c)

Figure 3 Optical textures of monomers (×200): (a) oily streaks texture of $\mathbf{M_1}$ at 150°C; (b) focal conic texture of $\mathbf{M_1}$ at 143°C; and (c) threaded texture of $\mathbf{M_2}$ at 162°C. [Color figure can be viewed in the online issue, which is available at www.interscience.wiley.com.]

spacer in the side groups). Figure 4 shows the effect of $\mathbf{M_2}$ concentration on the phase transition temperatures of the polymers. T_g and T_i of the polymers increased with increasing the concentration of $\mathbf{M_2}$

TABLE IV
Mesmorphic Properties of Polymers

Polymers	T_g (°C)	T_i (°C)	ΔT[a]	T_d (°C)[b]	Mesophase
$\mathbf{P_1}$	32.4	164.3	131.9	325.7	S_A
$\mathbf{P_2}$	33.9	168.5	134.6	330.5	Ch
$\mathbf{P_3}$	36.2	175.4	139.6	335.6	Ch
$\mathbf{P_4}$	41.5	191.7	150.2	336.3	Ch
$\mathbf{P_5}$	46.7	210.2	163.5	341.3	Ch
$\mathbf{P_6}$	48.3	225.6	177.3	346.7	Ch
$\mathbf{P_7}$	52.4	239.4	187.0	378.2	N

S, smectic; Ch, cholesteric; N, nematic.
[a] Mesophase temperature range (T_i–T_g).
[b] Temperature at which 5% weight loss occurred.

units. The reason is that the stronger rigidity of the mesogenic unit or the shorter length of the flexible spacer in the side groups for $\mathbf{M_2}$ units. As shown in Table IV, T_g increased from 32.4°C for $\mathbf{P_1}$ to 52.4°C for $\mathbf{P_7}$ when increased from 0 to 100 mol %. Similar to T_g, the copolymer composition affected T_i of $\mathbf{P_2}$–$\mathbf{P_6}$. With increasing the concentration of $\mathbf{M_2}$, T_i increased from 168.5°C for $\mathbf{P_2}$ to 225.6°C for $\mathbf{P_6}$. Moreover, $\mathbf{P_1}$–$\mathbf{P_7}$ revealed wide mesophase temperature ranges (ΔT), and ΔT increased from 131.9 to 187.0°C because T_i increased greater than T_g.

POM results showed that all obtained polymers displayed an enantiotropic LC phase. $\mathbf{P_1}$ exhibited the fan-shaped textures of smectic A (S_A) phase, in this case the smetic layer are basically perpendicular to the substrate plane. However, the cholesteric phase, exhibited for $\mathbf{M_1}$, did not appear. This indicated that the polymer chains hindered the formation of cholesteric helical supermolecular structure of the mesogens, and the mesogenic moieties were ordered in a smectic orientation with their centers of gravity in planes. It was also documented that the mesophase formed by side-chain LCPs was more organized than that exhibited by the corresponding

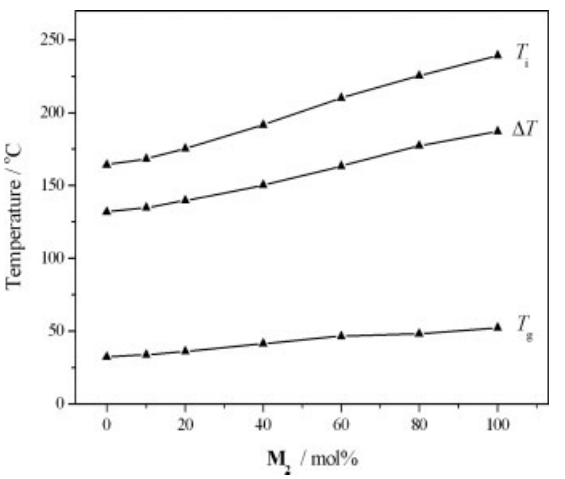

Figure 4 Effect of $\mathbf{M_2}$ concentration on the phase transition temperatures of polymers.

monomer. Moreover, the LCPs with siloxane macromolecular chains tend to form lower order smectic phase. The copolymers $\mathbf{P_2}$–$\mathbf{P_6}$ exhibited cholesteric Grandjean texture, this indicated the cholesteric copolymers could be obtained by the copolymerization of the chrial mesogenic monomer and nematic monomer. $\mathbf{P_7}$ exhibited nematic-threaded texture similar to the corresponding $\mathbf{M_2}$. The optical textures of $\mathbf{P_1}$, $\mathbf{P_2}$, and $\mathbf{P_7}$ are shown in Figure 5(a–c).

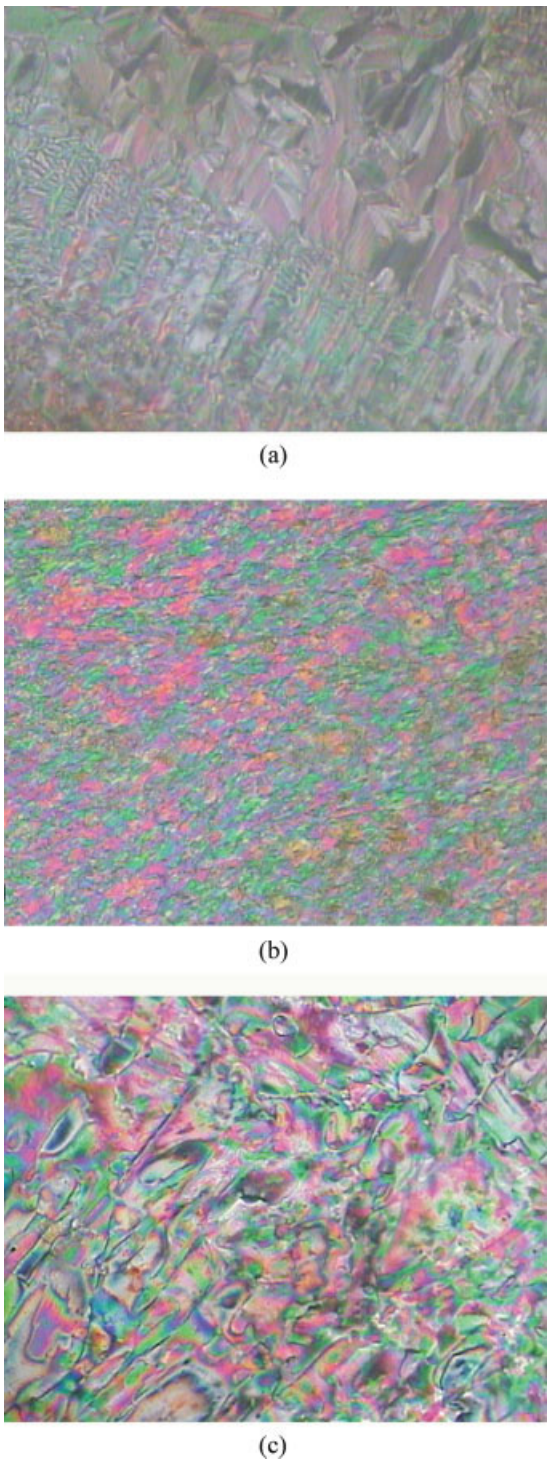

Figure 5 Optical textures of polymers (×200): (a) fan-shaped texture at 155°C for $\mathbf{P_1}$; (b) Grandjean texture at 161°C for $\mathbf{P_2}$; and (c) threaded texture at 196°C for $\mathbf{P_7}$. [Color figure can be viewed in the online issue, which is available at www.interscience.wiley.com.]

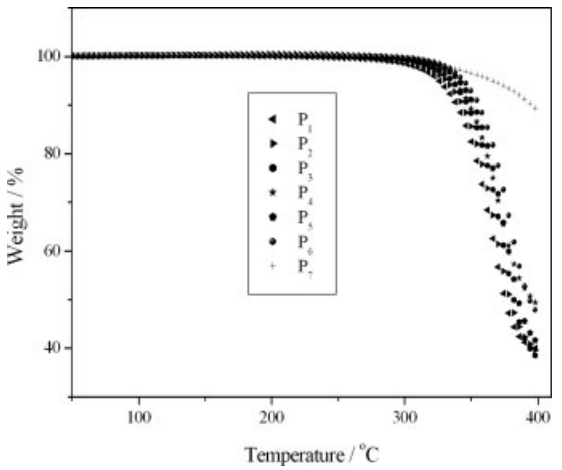

Figure 6 TGA curves of the polymers.

The thermal stability of $\mathbf{P_1}$–$\mathbf{P_7}$ is detected with TGA. The corresponding data are shown in Table IV. TGA curve of the polymers is shown as an example in Figure 6. TGA results showed that the temperatures at which 5% weight loss occurred (T_d) were greater than 320°C for $\mathbf{P_1}$–$\mathbf{P_7}$; this showed that the obtained side-chain LCPs had good thermal stability.

CONCLUSIONS

New chiral LC monomer $\mathbf{M_1}$ and nematic monomer $\mathbf{M_2}$, and a series of side-chain cholesteric copolymers containing menthyl groups were prepared and characterized. $\mathbf{M_1}$ revealed the oily streak texture, finger print texture, and focal conic texture of the cholesteric phase. $\mathbf{M_2}$ revealed the threaded texture and schlieren texture of the nematic phase. The homopolymers $\mathbf{P_1}$ and $\mathbf{P_7}$ exhibited the fan-shaped textures of a S_A phase and the threaded texture of the nematic phase, respectively. The copolymers $\mathbf{P_2}$–$\mathbf{P_6}$ derived from mesogenic menthyl groups and nematic units displayed the Grandjean texture of the cholesteric phase. For $\mathbf{P_2}$–$\mathbf{P_6}$, T_g, T_i, and ΔT increased with increasing the concentration of $\mathbf{M_2}$ in the copolymers. All of the obtained polymers displayed very good thermal stability.

References

1. Shibaev, V. P.; Plate, N. A. Adv Polym Sci 1984, 60, 174.
2. Belayev, S. V.; Schadt, M. I.; Funfschiling, J.; Malimoneko, N. V.; Schmitt, K. Jpn J Appl Phys 1990, 29, L634.
3. Bunning, T. J.; Kreuzer, F. H. Trends Polym Sci 1995, 3, 318.
4. Kricheldorf, H. R.; Sun, S. J.; Chen, C. P.; Chang, T. C. J Polym Sci Part A: Polym Chem 1997, 35, 1611.

5. Sapich, B.; Stumpe, J.; Kricheldorf, H. R. Macromolecules 1998, 31, 1016.
6. Rukmani, S.; Ganga, R. J Polym Sci Part A: Polym Chem 2001, 39, 1743.
7. Mruk, R.; Zentel, R. Macromolecules 2002, 35, 185.
8. Hu, J. S.; Zhang, B. Y.; Jia, Y. G.; Wang, Y. Polym J 2003, 35, 160.
9. Lin, Q.; Pasatta, J.; Long, T. E. J Polym Sci Part A: Polym Chem 2003, 41, 2512.
10. Oaki, Y.; Imai, H. J Am Chem Soc 2004, 126, 9271.
11. Wang, L.; Wang, X.; Huang, L. J Appl Polym Sci 2004, 92, 213.
12. Kakuchi, R.; Sakai, R.; Otsuka, I.; Satoh, T. Macromolecules 2005, 38, 9441.
13. Abraham, S.; Paul, S.; Narayan, G.; Prasad, S. K.; Jayaraman, N.; Das, S. Adv Funct Mater 2005, 15, 1579.
14. Brettar, J; Bürgi, T.; Donnio, B.; Guillon, D.; Klappert, R. Adv Funct Mater 2006, 16, 260.
15. Sahin, Y. M. C.; Serhatli, I. E.; Menceloglu, Y. Z. J Appl Polym Sci 2006, 102, 1915.
16. Liu, J. H.; Yang, P. C.; Chiu, Y. H.; Suda, Y. J Polym Sci Part A: Polym Chem 2007, 45, 2026.
17. Hsiue, G. H.; Chen, J. H. Macromolecules 1995, 28, 4366.
18. Hsu, C. S.; Chu, P. H.; Chang, H. L.; Hseih, T. H. J Polym Sci Part A: Polym Chem 1997, 35, 2793.
19. Mihaea, T.; Nozuhiro, K.; Funaki, K.; Koide, N. Polym J 1997, 29, 309.
20. Chiang, W. Y.; Hong, L. D. J Polym Sci Part A: Polym Chem 2000, 38, 1609.
21. Hu, J. S.; Zhang, B. Y.; He, X. Z.; Cheng, C. S. Liq Cryst 2004, 31, 1357.
22. Soltysiak, J. T.; Czupryński, K.; Drzewiński, W. Polym Int 2006, 55, 273.
23. Zhang, B. Y.; Hu, J. S.; Yang, L. Q.; He, X. Z.; Liu, C. Eur Polym J 2007, 43, 2017.
24. Finkelmann, H.; Koldehoff, J.; Ringsdorf, H. Angew Chem Int Ed Engl 1978, 17, 935.
25. Bobrovsky, A. Y.; Boiko, N. I.; Shaumburg, K.; Shibaev, V. P. Colloid Polym Sci 2000, 278, 671.
26. Bobrovsky, A. Y.; Boiko, N. I.; Shibaev, V. P. Liq Cryst 2000, 27, 1381.
27. Bobrovsky, A. Y.; Boiko, N. I.; Shibaev, V. P. Liq Cryst 2001, 28, 919.
28. Lee, Y. K.; Onimura, K.; Tsutsumi, H.; Oishi, T. J Polym Sci Part A: Polym Chem 2000, 38, 4315.
29. Yoshioka, T.; Zahangir, M.; Ogata, T.; Kurihara, S. Liq Cryst 2004, 31, 1285.
30. Hu, J. S.; Zhang, B. Y.; Pan, W.; Zhou, A. J Liq Cryst 2005, 32, 441.
31. Du, B. G.; Hu, J. S.; Zhang, B. Y.; Xiao, L. J.; Wei, K. Q. J Appl Polym Sci 2006, 102, 5559.
32. Liu, J. H.; Yang, P. C. Polymer 2006, 47, 4925.
33. Hu, J. S.; Zhang, B. Y.; Feng, Z. L.; Wang, H. G.; Zhou, A. J. J Appl Polym Sci 2001, 80, 2335.
34. Hu, J. S.; Zhang, B. Y.; Zhou, A. J.; Du, B. G.; Yang, L. Q. J Appl Polym Sci 2006, 100, 4234.
35. Hu, J. S.; Zhang, B. Y.; Liu, L. M.; Meng, F. B. J Appl Polym Sci 2003, 89, 3944.